Synthesis, Structure Determination, and Hydrogen Sorption Studies of New Metal−Organic Frameworks Using Triazole and Naphthalenedicarboxylic Acid

Hyunsoo Park,[†,‡] James F. Britten,[§] Ulrich Mueller,[||] JeongYong Lee,[#] Jing Li,[#] and
John B. Parise*[,†,‡,⊥]

Department of Chemistry and Center for Environmental Molecular Science, State University of New York at Stony Brook, Stony Brook, New York 11794, Department of Chemistry, McMaster University, Hamilton, ON, L8S 4M1 Canada, BASF Aktiengesellschaft, Chemicals Research & Engineering, D-67056, Ludwigshafen, Germany, Department of Chemistry and Chemical Biology, Rutgers University, Piscataway, New Jersey 08854, and Department of Geosciences, State University of New York at Stony Brook, Stony Brook, New York 11794

Received October 6, 2006. Revised Manuscript Received January 10, 2007

Two new metal−organic framework compounds were synthesized under solvothermal conditions using Zn^{2+} ion, 1,2,4-triazole (TRZ), and 1,4- and 2,6-naphthalenedicarboxylic acids (NDC): $Zn_4(TRZ)_4(1,4\text{-}NDC)_2{\cdot}2DMF{\cdot}2H_2O$ (**1**) and $Zn_4(TRZ)_4(2,6\text{-}NDC)_2{\cdot}2DMF{\cdot}4H_2O$ (**2**). Their crystal structures were characterized by single-crystal X-ray diffraction. Structure **1** crystallizes in the $P2_1/n$ space group with $a = 13.609(2)$ Å, $b = 27.181(5)$ Å, $c = 13.617(3)$ Å, $\beta = 92.46(1)$ °, $V = 5032.4(16)$ Å^3, and $Z = 4$. Structure **2** crystallizes in orthorhombic $Pna2_1$ space group with $a = 30.978(6)$ Å, $b = 12.620(3)$ Å, $c = 13.339(3)$ Å, $V = 5215(2)$ Å^3, and $Z = 4$. Both structures are analogues of the previously reported $Zn_4(TRZ)_4(1,4\text{-}BDC)_2{\cdot}16H_2O$ where the layers of Zn−triazole moieties are pillared by aromatic dicarboxylates to create 3-D open frameworks. Nitrogen sorption studies revealed that these structures have Brunaer−Emmett−Teller (BET) surface areas of 362.1−584.1 m^2/g. Hydrogen sorption experiments showed they can store 0.84−1.09 wt % of H_2 at 77 K and 1 atm. Although they do not contain large pores or surface areas, they possess the hydrogen sorption capacities comparable to those of highly porous metal−organic frameworks.

Introduction

Metal−organic frameworks (MOFs) constitute a new class of crystalline, porous materials whose structures are based on the linkage of metal ions with functionalized organic molecules. Through the extensive choice of metals and organic ligands, a wide range of new structures have been prepared and their physical properties have been examined.[1−7] Many MOFs have been explored for their gas sorption characteristics to investigate their potential applications as hydrogen storage materials.[8−22] Work was initially geared toward synthesizing MOFs with large surface area and high porosity,[14,23,24] however, recent research has found that there is no clear relationship between H_2 capacity and surface area.[15,16,20,25] Several strategies to increase the H_2 uptake of MOF have been suggested[26,27] on the basis of the results from inelastic neutron scattering,[19,28] powder and single-crystal

---

* To whom correspondence should be addressed. E-mail: jparise@notes.cc.sunysb.edu.
[†] Department of Chemistry, State University of New York at Stony Brook.
[‡] Center for Environmental Molecular Science, State University of New York at Stony Brook.
[§] McMaster University
[||] BASF Aktiengesellschaft.
[#] Rutgers University.
[⊥] Department of Geosciences, State University of New York at Stony Brook.

(1) Eddaoudi, M.; Moler, D. B.; Li, H. L.; Chen, B. L.; Reineke, T. M.; O'Keeffe, M.; Yaghi, O. M. *Acc. Chem. Res.* **2001**, *34*, 319.
(2) James, S. L. *Chem. Soc. Rev.* **2003**, *32*, 276.
(3) Rowsell, J. L. C.; Yaghi, O. M. *Microporous Mesoporus Mater.* **2004**, *73*, 3.
(4) Kitagawa, S.; Kitaura, R.; Noro, S. *Angew. Chem., Int. Ed.* **2004**, *43*, 2334.
(5) Rao, C. N. R.; Natarajan, S.; Vaidhyanathan, R. *Angew. Chem., Int. Ed.* **2004**, *43*, 1466.
(6) Ferey, G.; Mellot-Draznieks, C.; Serre, C.; Millange, F. *Acc. Chem. Res.* **2005**, *38*, 217.
(7) Mueller, U.; Schubert, M.; Teich, F.; Puetter, H.; Schierle-Arndt, K.; Pastre, J. *J. Mater. Chem.* **2006**, *16*, 626.
(8) Chen, B. L.; Ma, S. Q.; Zapata, F.; Lobkovsky, E. B.; Yang, J. *Inorg. Chem.* **2006**, *45*, 5718.
(9) Chen, B. L.; Ockwig, N. W.; Millward, A. R.; Contreras, D. S.; Yaghi, O. M. *Angew. Chem., Int. Ed.* **2005**, *44*, 4745.
(10) Dybtsev, D. N.; Chun, H.; Kim, K. *Angew. Chem., Int. Ed.* **2004**, *43*, 5033.
(11) Chun, H.; Dybtsev, D. N.; Kim, H.; Kim, K. *Chem. Eur. J.* **2005**, *11*, 3521.
(12) Dinca, M.; Yu, A. F.; Long, J. R. *J. Am. Chem. Soc.* **2006**, *128*, 8904.
(13) Fang, Q. R.; Zhu, G. S.; Xue, M.; Zhang, Q. L.; Sun, J. Y.; Guo, X. D.; Qiu, S. L.; Xu, S. T.; Wang, P.; Wang, D. J.; Wei, Y. *Chem. Eur. J.* **2006**, *12*, 3754.
(14) Ferey, G.; Mellot-Draznieks, C.; Serre, C.; Millange, F.; Dutour, J.; Surble, S.; Margiolaki, I. *Science* **2005**, *309*, 2040.
(15) Kesanli, B.; Cui, Y.; Smith, M. R.; Bittner, E. W.; Bockrath, B. C.; Lin, W. B. *Angew. Chem., Int. Ed.* **2005**, *44*, 72.
(16) Lin, X.; Jia, J.; Zhao, X.; Thomas, K. M.; Blake, A. J.; Walker, G. S.; Champness, N. R.; Hubberstey, P.; Schröder, M. *Angew. Chem., Int. Ed.* **2006**, *45*, 7358.
(17) Pan, L.; Parker, B.; Huang, X. Y.; Olson, D. H.; Lee, J.; Li, J. *J. Am. Chem. Soc.* **2006**, *128*, 4180.
(18) Pan, L.; Sander, M. B.; Huang, X. Y.; Li, J.; Smith, M.; Bittner, E.; Bockrath, B.; Johnson, J. K. *J. Am. Chem. Soc.* **2004**, *126*, 1308.
(19) Rosi, N. L.; Eckert, J.; Eddaoudi, M.; Vodak, D. T.; Kim, J.; O'Keeffe, M.; Yaghi, O. M. *Science* **2003**, *300*, 1127.
(20) Sun, D. F.; Ma, S. Q.; Ke, Y. X.; Collins, D. J.; Zhou, H. C. *J. Am. Chem. Soc.* **2006**, *128*, 3896.

10.1021/cm0623918 CCC: $37.00 © 2007 American Chemical Society
Published on Web 02/21/2007

Table 1. Crystallographic Data and Structure Refinement Details

	structure **1**	structure **2**
empirical formula	$C_{38}H_{40}N_{14}O_{13}Zn_4$	$C_{38}H_{42}N_{14}O_{14}Zn_4$
formula weight	1156.27	1172.27
collection temp (K)	100(2)	100(2)
wavelength (Å)	0.71073	0.49594
space group	$P2_1/n$	$Pna2_1$
unit cell dimensions (Å, °)	$a = 13.609(2)$ $b = 27.781(5)$ $c = 13.617(3)$ $\beta = 92.46(1)$	$a = 30.978(6)$ $b = 12.620(3)$ $c = 13.339(3)$
volume (Å^3)	5032.4(16)	5215(2)
Z, calcd density (g/cm^3)	4, 1.526	4, 1.493
absorption coefficient (mm^{-1})	1.955	0.997
F(000)	2336	2368
crystal size (mm)	0.10 × 0.07 × 0.07	0.04 × 0.03 × 0.03
θ range for data collection (°)	3.3−65.2	1.4−16.95
index ranges	$-16 \leq h \leq 15$ $0 \leq k \leq 31$ $0 \leq l \leq 16$	$-36 \leq h \leq 36$ $-14 \leq k \leq 14$ $-13 \leq l \leq 15$
total reflections	8494	19004
independent reflections	8314 [R(int) = 0.000]	7114 [R(int) = 0.057]
absorption correction	TWINABS	SADABS
max & min transmission	0.855 & 0.621	0.926 & 0.833
refinement method	full-matrix least-squares on F^2	full-matrix least-squares on F^2
data/restraints/parameters	8314/0/295	7114/2/346
goodness-of-fit	0.95	1.24
final R [$I > 2\sigma$(I)]	$R1 = 0.1033$ w$R2 = 0.2347$	$R1 = 0.1103$ w$R2 = 0.2743$
R (all data)	$R1 = 0.2650$ w$R2 = 0.2742$	$R1 = 0.1170$ w$R2 = 0.2837$
largest difference peak and hole (eÅ^{-3})	1.23 and −1.79	2.38 and −1.91

neutron diffraction,[29,30] and Monte Carlo simulations.[31] Since H_2 molecules seem to interact strongly with metal-based binding sites, it may be advantageous to introduce smaller pore sizes and coordinatively unsaturated metal centers in MOFs to enhance their H_2 sorption abilities.[11,15,20]

Various approaches have been developed to create MOFs with well-defined pores and high framework stability. One of the more recent methods is to apply pillar ligands to bridge 2-D layers. This type of framework consists of two types of organic linkers, typically aromatic dicarboxylate and diamine, where the 2-D grids formed by metal ions and amines are connected by dicarboxylates through metal−O bonds. These frameworks offer several attractive features such as structural rigidity and high porosity, and many MOFs using this strategy have been reported.[10,11,25,32−34] For example, Kim and co-workers systematically prepared a series of 3-D frameworks on the basis of Zn−DABCO/4,4′-bypyridyl-aromatic dicarboxylates (DABCO = 4-diazabicyclo[2.2.2]-octane).[10,11] These materials were found to adsorb 1.7−2.1 wt % of H_2 at 1 atm and 77 K.

We have synthesized two new MOFs on the basis of the above approach by using 1,2,4-triazole (TRZ) and aromatic dicarboxylates. This work is an extension of an MOF, $Zn_4(H_2O)_2(TRZ)_4(1,4\text{-BDC})_2\cdot14H_2O$ (1,4-BDC = 1,4-benzenedicarboxylate), which we have previously reported.[34] By substituting 1,4-BDC with 1,4- and 2,6-naphthalenedicarboxylates (NDC), we obtained two new open frameworks that exhibit the same structural features as the original one. In this report, we present the synthesis and structural characterization of $Zn_4(TRZ)_4(1,4\text{-NDC})_2\cdot2DMF\cdot2H_2O$ (**1**) and $Zn_4(TRZ)_4(2,6\text{-NDC})_2\cdot2DMF\cdot4H_2O$ (**2**). In addition, the gas-sorption properties of **1** and **2** as well as the previously described $Zn_4(H_2O)_2(TRZ)_4(1,4\text{-BDC})_2\cdot14H_2O$ (**3**) are given and their H_2 sorption characteristics are discussed.

Experimental Section

Synthesis. Both compounds were synthesized under solvothermal conditions using a 23-mL Teflon-lined Parr autoclave. Starting materials include zinc nitrate hexahydrate ($Zn(NO_3)_2\cdot6H_2O$, 99%, Alfa-Aesar), 1,2,4-triazole (TRZ, 99%, Alfa-Aesar), 1,4-naphthalenedicarboxylic acid (1,4-NDC, 95%, Sigma-Aldrich), 2,6-naphthalenedicarboxylic acid (2,6-NDC, 98%, Sigma-Aldrich), and dimethylformamide (DMF, 99.9%, Sigma-Aldrich). The C, H, and N analyses of the products were performed by Galbraith Laboratories.

$Zn_4(TRZ)_4(1,4\text{-NDC})_2\cdot2DMF\cdot2H_2O$ (Structure 1). In a typical reaction, $Zn(NO_3)_2\cdot6H_2O$ (0.30 g, 100 mmol), TRZ (0.07 g, 100 mmol), and 1,4-NDC (0.11 g, 50 mmol) were added to DMF (5.00

---

(21) Zhao, X. B.; Xiao, B.; Fletcher, A. J.; Thomas, K. M.; Bradshaw, D.; Rosseinsky, M. J. *Science* **2004**, *306*, 1012.

(22) Fletcher, A. J.; Thomas, K. M.; Rosseinsky, M. J. *J. Solid State Chem.* **2005**, *178*, 2491.

(23) Li, H.; Eddaoudi, M.; O'Keeffe, M.; Yaghi, O. M. *Nature* **1999**, *402*, 276.

(24) Rowsell, J. L. C.; Millward, A. R.; Park, K. S.; Yaghi, O. M. *J. Am. Chem. Soc.* **2004**, *126*, 5666.

(25) Chen, B. L.; Liang, C. D.; Yang, J.; Contreras, D. S.; Clancy, Y. L.; Lobkovsky, E. B.; Yaghi, O. M.; Dai, S. *Angew. Chem., Int. Ed.* **2006**, *45*, 1390.

(26) Rowsell, J. L. C.; Yaghi, O. M. *Angew. Chem., Int. Ed.* **2005**, *44*, 4670.

(27) Rowsell, J. L. C.; Yaghi, O. M. *J. Am. Chem. Soc.* **2006**, *128*, 1304.

(28) Rowsell, J. L. C.; Eckert, J.; Yaghi, O. M. *J. Am. Chem. Soc.* **2005**, *127*, 14904.

(29) Spencer, E. C.; Howard, J. A. K.; McIntyre, G. J.; Rowsell, J. L. C.; Yaghi, O. M. *Chem. Commun.* **2006**, 278.

(30) Yildirim, T.; Hartman, M. R. *Phys. Rev. Lett.* **2005**, 95.

(31) Frost, H.; Duren, T.; Snurr, R. Q. *J. Phys. Chem. B* **2006**, *110*, 9565.

(32) Kitaura, R.; Iwahori, F.; Matsuda, R.; Kitagawa, S.; Kubota, Y.; Takata, M.; Kobayashi, T. C. *Inorg. Chem.* **2004**, *43*, 6522.

(33) Ma, B. Q.; Mulfort, K. L.; Hupp, J. T. *Inorg. Chem.* **2005**, *44*, 4912.

(34) Park, H.; Moureau, D. M.; Parise, J. B. *Chem. Mater.* **2006**, *18*, 525.

g, 82 mmol). The reactants were stirred for 1 h prior to heating at 120 °C for 4 days. After reaction, the products were filtered, were washed with ethanol, and were dried in air. Small, light-yellow block-shaped crystals were recovered. Elemental analysis (%) calcd for $C_{38}H_{38}N_{14}O_{12}Zn_4$: C, 39.9; H, 3.4; N, 17.1. Found: C, 40.1; H, 3.6; N, 17.4.

$Zn_4(TRZ)_4(2,6\text{-}NDC)_2\cdot 2DMF\cdot 4H_2O$ (Structure **2**). $Zn(NO_3)_2\cdot 6H_2O$ (0.30 g, 100 mmol), TRZ (0.07 g, 100 mmol), and 2,6-NDC (0.11 g, 50 mmol) were mixed with DMF (5.00 g, 82 mmol). After stirring for 1 h, the reactants were heated at 150 °C for 3 days. Upon filtering, aggregates of colorless plates were obtained. Elemental analysis (%) calcd for $C_{38}H_{42}N_{14}O_{14}Zn_4$: C, 38.6; H, 3.6; N, 16.6. Found: C, 41.2; H, 3.8; N, 17.3.

Crystal Structure Determination. *Structure **1***. Data collection was carried out using a Bruker P4 diffractometer with Mo Kα radiation equipped with a SMART 1K CCD detector at Department of Chemistry, McMaster University. The data were collected at 100 K with an exposure time of 60 s per frame and a detector distance of 4.994 cm. Nine different sections of frames were measured with a stepsize of 0.36° in ω and φ. Using GEMINI,[35] the reflections were indexed, and the twin law was found to be [0 0 1/0 −1 0/1 0 0], which corresponds to a rotation about (101) direction. The ratio of the two twin components was estimated to be approximately 3:1. Both twin components were integrated with SAINT,[36] and an absorption correction was applied using TWINABS.[37] The structure was solved by direct method and subsequent difference Fourier syntheses and then was refined with SHELXTL[38] software. The hydrogen atoms were added using geometrical constraints (HFIX command). Because of the strong disorder of water and DMF in the channels, the amount and position of the solvents could not be accurately determined from the structural refinement.

*Structure **2***. Data collection and structure determination were carried out at 15-ID ChemMatCARS beamline at Advanced Photon Source, Argonne National Laboratory. The data were collected at 100 K with wavelength of 0.4959 Å and an exposure time of 2 s per frame and a detector distance of 6.0 cm. A randomly oriented region of reciprocal spaces was examined to a resolution of 0.75 Å. Two major sections of frames were collected with a step size of 0.30° in ω and ϕ. The raw intensity data were collected and integrated with software packages SMART[39] and SAINT,[36] and then an empirical absorption correction was applied using SADABS.[40] The final unit cell parameters were determined from 1024 strong reflections after integration. The crystal structures were solved via direct method and were refined assuming anisotropic displacement parameters for Zn and O atoms with SHELXTL.[38] Zinc atoms were located first and the remaining atoms (O, C, N) were found from subsequent Fourier difference map synthesis. The hydrogen atoms were added to their ideal positions using HFIX command. The details of the crystal structures are given in Table 1.

Thermal Analysis. Thermogravimetric analysis (TGA) was performed using a Netzsch STA 449C instrument. Each sample was heated from room temperature (RT) to 800 °C in air with a heating rate of 5.0 °C/min. The TGA plots are given in Figure 1.

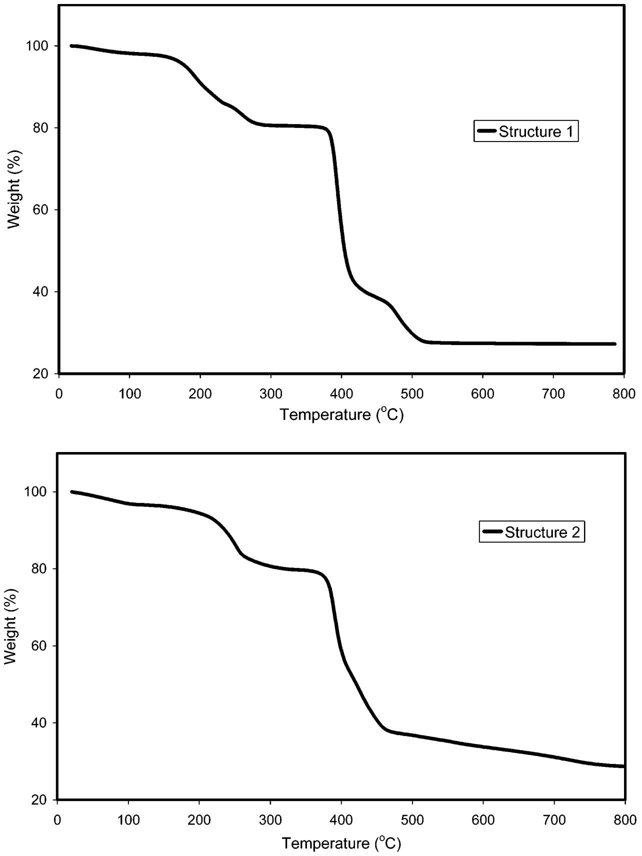

Figure 1. TGA plots of structures **1** and **2**.

*Structure **1***. The first event occurs between RT and 320 °C, which corresponds to the loss of water DMF molecules. Once all solvent molecules are evaporated, the framework starts to collapse, giving amorphous solid as a final product. The observed weight loss of solvents is slightly higher than the calculated value (observed: 20.0%, calculated: 14.4%) probably because the exact amount of solvents in the structure could not be identified from X-ray data because of disorder.

*Structure **2***. The removal of water and DMF molecules is characterized by the events between RT and 300 °C (calcd: 18.6%, obs: 20.0%). The framework subsequently collapses between 360 and 600 °C.

Gas Sorption Measurements. Nitrogen sorption experiments were carried out with a Micrometrics ASAP2010 volumetric gas sorption instrument. Prior to N_2 isotherm measurements at 77 K, samples were outgassed under a high vacuum (less than 10^{-5} Torr) at 150−200 °C overnight. About 70−80 mg of sample was weighed before and after the degassing procedure to confirm the evacuation of the solvents. The high-resolution hydrogen gas adsorption−desorption measurement for **1** was performed using an automated micropore gas analyzer Autosorb-1 MP (Quantachrome Instruments) at Department of Chemistry and Chemical Biology, Rutgers University. The hydrogen sorption isotherms were collected in a relative pressure range from 10^{-4} to 1 atm at 77 K. The cryogenic temperature was controlled using liquid nitrogen at 77 K. The initial outgassing process for **1** was carried out under vacuum at 150 °C for 18 h. About 70 mg of degassed sample was used and the weight of the sample was recorded before and after outgassing to confirm the removal of all guest molecules. A total analysis time was ca. 9 h for hydrogen sorption. The purity of hydrogen gas used was 5.0 UHP grade (99.999%). Hydrogen sorption properties were analyzed using Autosorb v1.50 software. The H_2 sorption isotherms of **2** and $Zn_2(TRZ)_2(1,4\text{-}BDC)$ (**3**) were recorded using an Autosorb instrument at BASF, Germany, using similar conditions as the

---

(35) Sparks, R. A. *GEMINI*, 1.02, Twinning Solution Program Suite; Bruker-AXS: Madison, WI, 2000.
(36) *SAINT*, 6.2; Bruker-AXS: Madison, WI, 2002.
(37) Sheldrick, G. M. *TWINABS*; Bruker-AXS: Madison, WI, 2002.
(38) Sheldrick, G. M. *SHELXTL*, 6.10; Bruker-AXS: Madison, WI, 2000.
(39) *SMART*, 5.625; Bruker-AXS: Madison, WI, 2001.
(40) Sheldrick, G. M. *SADABS*, a program for the Siemens Area Detector Absorption Program; Bruker-AXS: Madison, WI, 2001.

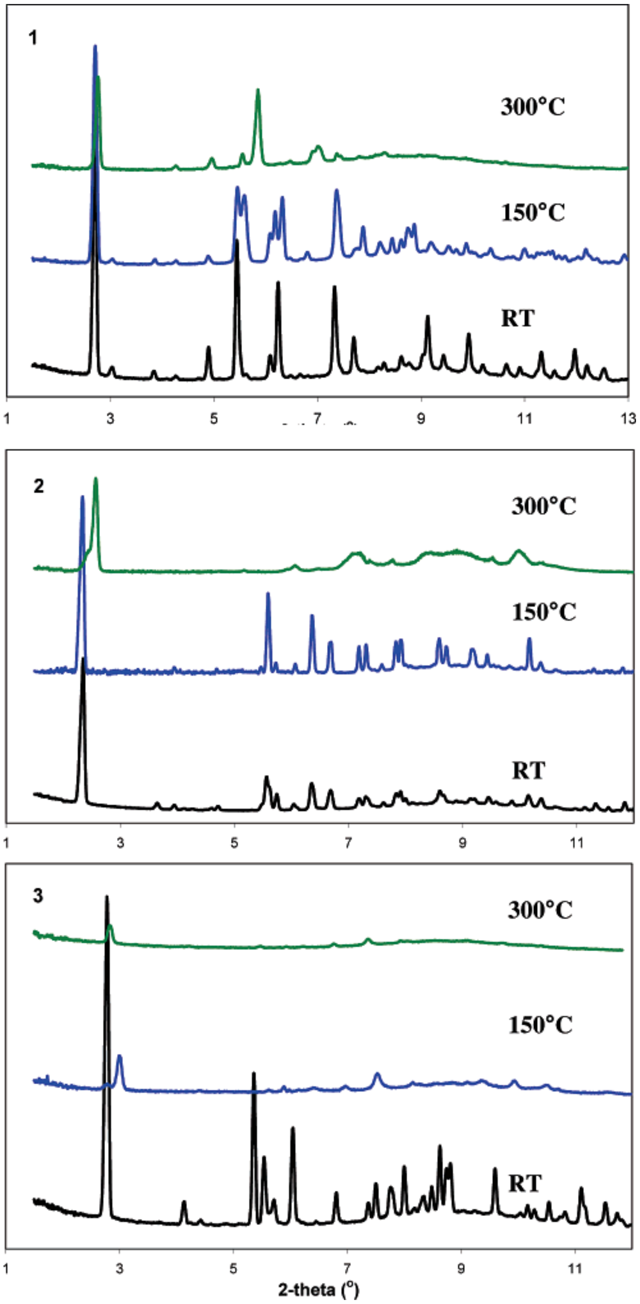

Figure 2. High-temperature powder XRD plots of structures **1**−**3**.

studies of **1** and **2**. Both samples were evacuated prior to the measurements at 150−200 °C overnight. All H_2 isotherms were measured at 77 K.

Powder X-ray Diffraction. High-temperature powder X-ray diffraction was carried out at X7A beamline, National Synchrotron Light Source, Brookhaven National Laboratory. Each powdered sample was placed in a 0.5-mm quartz capillary. The X-ray diffraction (XRD) was measured at RT, 150 °C, and 300 °C in the 2θ range of 1.50−30.00° with a step size of 0.01°. Typically, the sample was equilibrated for ∼20 min at each measured temperature, and XRD data were collected for 2−3 h using a monochromatic X-ray ($\lambda = 0.6482$ Å) provided by a bent Si(111) monochromator and a gas-proportional position-sensitive detector. The XRD patterns are shown in Figure 2.

Results and Discussion

Structural Characterization. Both structures **1** and **2** were prepared under solvothermal conditions using DMF as a solvent. They were obtained as aggregates of very small crystals. Although many experiments were carried out to improve the size and quality of the crystals by systematically varying several reaction parameters (reactant ratio, solvent, temperature, and reaction time), single crystals of sufficient quality could not be obtained to produce clear and precise crystallographic data. The presence of a tetragonal pseudosymmetry also adds to the difficulties in accurate characterization of both structures. Weak, diffused diffraction spots suggested that a true symmetry is in fact monoclinic and orthorhombic for **1** and **2**, respectively. Nevertheless, the structural models presented in this work show sufficient resolution and quality to describe the details of the main frameworks. The crystal chemistry of these structures is consistent with that of previously reported analogue,[34] providing confidence that the structures are correct. The syntheses of different metal analogues were also attempted using Ni^{2+}, Co^{2+}, and Cu^{2+}, but none of the reactions have been successful so far in producing high-quality crystals.

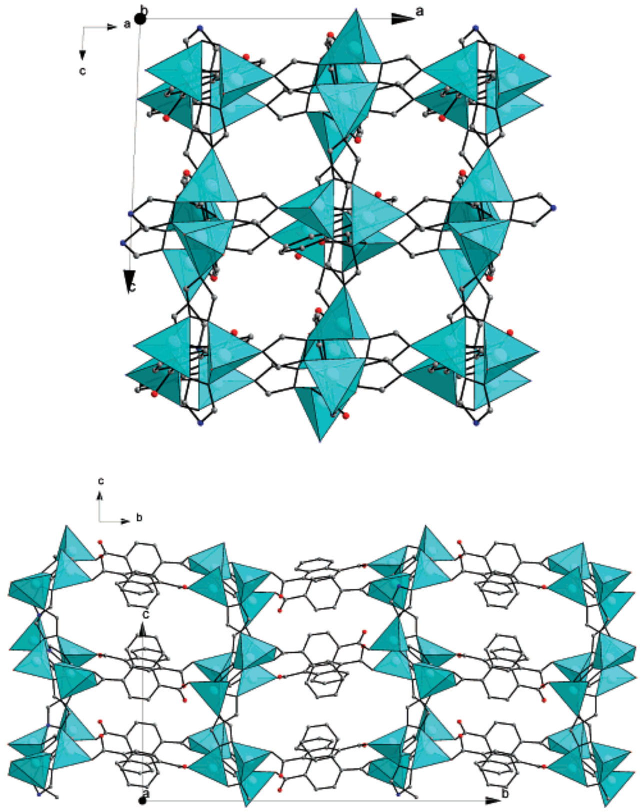

Figure 3. Crystal structure of **1** viewed along the *b*-axis (above) and *a*-axis (below). The 2-D grid formed by Zn polyhedra (blue) and TRZ are pillared by 1,4-NDC. Hydrogen atoms, water, and DMF are omitted for clarity.

The crystal structure of $Zn_4(TRZ)_4(1,4\text{-}NDC)_2\cdot 2DMF\cdot 2H_2O$ (**1**) is shown in Figure 3. The asymmetric unit consists of four crystallographically independent Zn atoms, which are coordinated to three N atoms from three different triazole moieties and one O atom from a dicarboxylate group. The Zn−O and Zn−N bond distances are similar to the previously reported values,[10,11,34] ranging from 1.91 to 2.06 Å. The bond valence sum[41] around Zn2 is somewhat lower than the expected value of +2, however, Zn2 forms one long bond with the other O atom from the carboxylate (Zn2−O4 =

---

[41] (41) Brese, N. E.; O'Keefe, M. *Acta Crystallogr., Sect. B.* **1991**, *47*, 192.

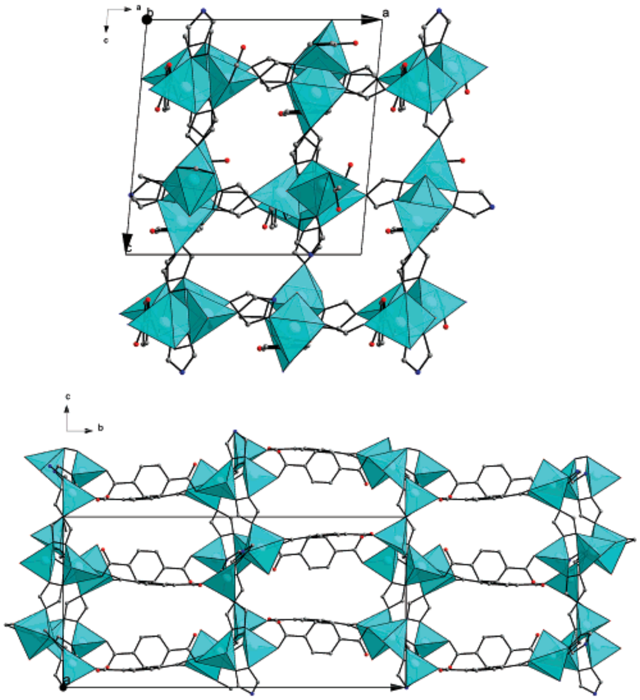

Figure 4. Crystal structure of **3** viewed along [010] direction (above) and [100] direction (below). Hydrogen atoms and water molecules are omitted for clarity.

2.49 Å). If this bond is included, the bond valence sum around Zn2 becomes more reasonable (1.9 vs 1.8). Structure **1** is a three-dimensional framework, which is derived from $Zn_4(TRZ)_4(1,4\text{-}BDC)_2$ (**3**)[34] (shown in Figure 4) by replacing the 1,4-BDC ligand with 1,4-NDC. Four dimers of Zn polyhedra are connected by four triazole molecules to create a layer consisting of eight-membered rings in the *ac*-plane. The dimensions of the ring are approximately 3.2 × 3.2 Å^2, considering the van der Waals radii,[42] which are comparable to those of **3** (3.1 × 3.1 Å^2). Two adjacent Zn-triazole layers are bridged by 1,4-NDC ligands to form channels along the *b*-axis. The 1,4-NDC ligands are oriented nearly perpendicular to each other with the angle of 81.6−98.2° between two naphthalene planes. Compared to **3**, these cavities in **1** are slightly smaller because of the additional phenyl group as well as the nonzero torsion angle between phenyl and carboxylates (82.0° and 5.8° for two 1,4-NDC groups). The difference in the cavity size between **1** and **3** can be also seen in the potential solvent accessible volume (39.0% and 44.3% for **1** and **3**, respectively).[43] Since two neighboring naphthalene rings are fairly close to each other (3.6−3.9 Å), there is a significant point-to-face $\pi-\sigma$ interaction present in the structure.[44] Inside the pores, noncoordinating solvents, water, and DMF are located. Water molecules are located near the dicarboxylates so that they can interact with each other via hydrogen bonding (O−H···O(carboxyl) = 2.7 Å).

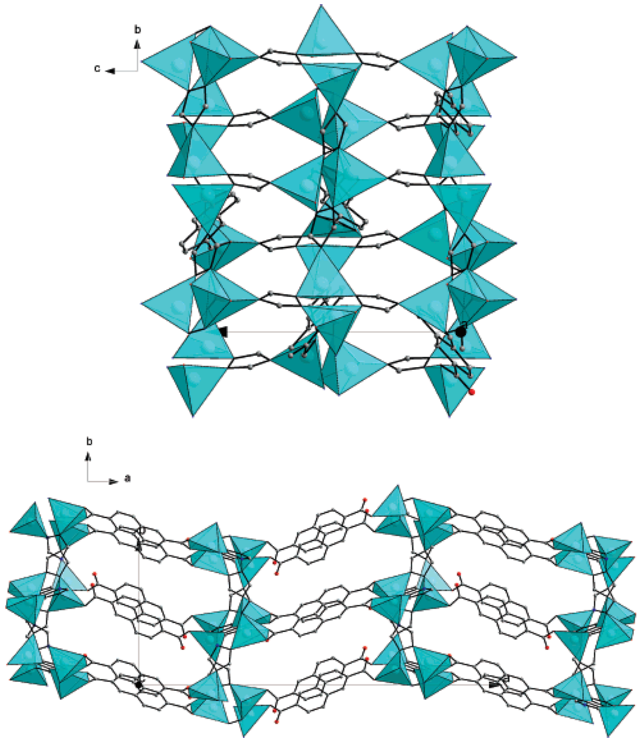

Figure 5. Crystal structure of **2** viewed down the [100] direction (above) and [001] direction (below). The pillared channels run zigzag along the *a*-axis. Hydrogen atoms and solvent molecules are omitted for clarity.

The crystal structure of $Zn_4(TRZ)_4(2,6\text{-}NDC)_2\cdot 2DMF\cdot 4H_2O$ (**2**) is depicted in Figure 5. Structure **2** can be described as an analogue of **1** and **3** by changing a dicarboxylate ligand. Zn1 and Zn2 atoms are tetrahedrally coordinated by bonding to three N and one carboxyl O atoms. Zn3 displays a trigonal bipyramidal geometry while Zn4 lies in a distorted octahedral coordination. Zn3 and Zn4 are weakly bonded to a carboxyl O atom and water, respectively (Zn3−O4 = 2.49 Å and Zn4−O11 = 2.48 Å). These long bonds are included as a part of the coordination environment around Zn3 and Zn4 to achieve bond valence sums closer to the value of 2 expected for Zn^{2+}. The eight-membered rings formed by Zn and triazole are similar to those in **1** and **3** with the dimensions of 3.2 × 3.2 Å^2, considering the van der Waals radii.[41] The Zn−triazole layers are again connected by 2,6-NDC to form channels which run zigzag along the *a*-axis. The length of pillared channels in **2** is greater, since a longer dicarboxylate linker is applied (10.1 Å vs 8.1 Å in **1**). The potential solvent-accessible volume in **2** is estimated to be 2151 Å^3 (41.2%),[43] which is slightly larger than that of **1**. There are no significant $\pi-\pi$ or $\pi-\sigma$ interactions between naphthalene rings as they are sufficiently away from each other (naphthalene−naphthalene distance = 5.0−6.1 Å).[44] DMF and water molecules are located inside the cavities. Hydrogen bonding between water and carboxyl oxygens are present (Ow···*O* = 2.8−2.9 Å).

As mentioned above, both structures **1** and **2** show a pseudotetragonal symmetry with two nearly equal axial dimensions and $\alpha = \beta = \gamma \approx 90°$. Attempts to solve the structures in higher symmetry settings were not successful. Powder XRD results did not provide a clear distinction between different symmetries. Structure **2** is best described in orthorhombic $Pna2_1$ space group whereas **1** and **3** crystallize in the monoclinic $P2_1/n$ space group. The deviations from tetragonal symmetry in all three structures can be attributed to the topology of the dicarboxylate ligand and the shape of the channels. In **1**, the asymmetrical shape of

---

(42) Bondi, A. *J. Phys. Chem.* **1964**, *68*, 441.
(43) Spek, A. L. *PLATON*, a multipurpose crystallographic tool; Utrecht University: Utrecht, the Netherlands, 2001.
(44) Janiak, C. *Dalton Trans.* **2000**, 3885.

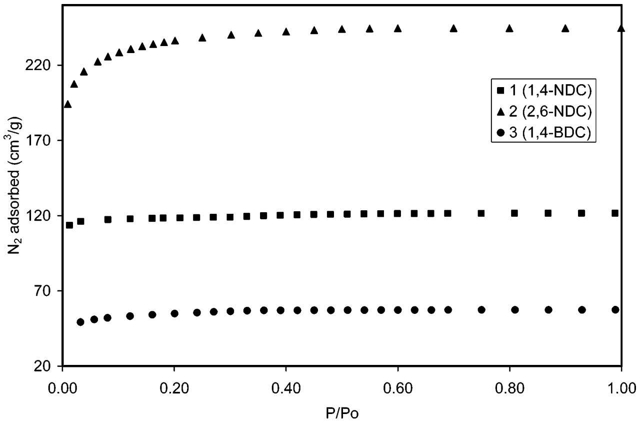

Figure 6. N_2 adsorption isotherm plots of **1** (squares), **2** (triangles), and **3** (circles) at 77 K.

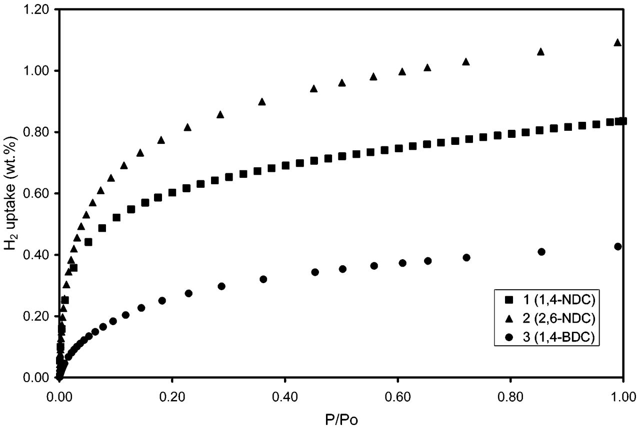

Figure 7. Adsorption isotherms for H_2 uptake of **1** (squares), **2** (triangles), and **3** (circles) at 77 K.

1,4-NDC does not allow the presence of a mirror plane in the (010) direction. In **3**, 1,4-BDC ligands are curved to connect two Zn−triazole layers to create sinusoidal channels, effectively removing the mirror plane. In **2**, the use of more symmetric 2,6-NDC leads to the additional mirror planes for the orthorhombic symmetry.

Powder XRD experiments were performed to test the stability of the structures at higher temperatures (Figure 2). Structure **1** is stable up to 300 °C, suggesting the framework is retained when the solvents are removed. For **2**, the framework seems to be stable at least up to 150 °C. At 300 °C, the intensities of the diffraction peaks become much weaker. Moreover, the position of (200) reflection (the first peak) is shifted, which implies the changes in the channels along the *a*-axis. Significant changes are observed in **3** between RT and 150 °C. The loss of diffraction peaks is probably due to the decomposition of the framework upon removal of solvent.

Gas-Sorption Studies. Gas-sorption properties of **1**−**3** were examined by measuring N_2 and H_2 adsorption isotherms at 77 K. The N_2 isotherms in Figure 6 display typical type-I adsorption characteristics. The Brunaer−Emmett−Teller (BET) surface areas of the solvent-free frameworks were estimated to be 362.1, 584.1, and 169.6 m^2/g for **1**, **2**, and **3**, respectively. Hydrogen adsorption isotherms were measured in the pressure range of 0 and 1 atm. The H_2 adsorption isotherms are given in Figure 7. The H_2 uptakes of **1**−**3** were 0.84, 1.11, and 0.43 wt %, respectively. When the H_2 sorption data were fitted with the Langmuir equation,[16] maximum adsorptions of 0.93, 1.18, and 0.49 wt % were predicted for **1**−**3**, respectively. Structure **3** displays the smallest surface area and the lowest H_2 capacity, despite the largest solvent-accessible volume among three structures. This may be explained by the fact that **3** may have lost its porosity upon the solvent removal. As seen in the high-temperature powder XRD, the crystallinity of **3** is already greatly reduced at 150 °C implying the partial collapse of the framework, while **1** and **2** maintain the structural integrity at the same temperature. It is not very clear why structure **3** is more susceptible to the decomposition at high temperature. Structure **3** contains two Zn centers (in octahedral and trigonal bipyramidal coordinations) which are bonded to the solvent H_2O molecules. The loss of coordinating H_2O may be responsible for the lack of thermal stability of **3**. Structure **1** does not contain any bound solvents, and structure **2** has only one H_2O which is loosely bonded to Zn4.

Both H_2 isotherms of **1** and **2** exhibit a very sharp initial slope which implies the presence of strong H_2 binding sites inside the cavities. It has been proposed that the H_2 uptake increases with decreasing pore size under low-pressure conditions because of the overlap of potential energy fields of the pore walls.[16] Therefore, it may be suggested that structures **1** and **2** possess a fairly high affinity toward H_2 molecules at a lower pressure range ($P/P_o < 0.4$) as they contain small pores. Moreover, the presence of coordinatively unsaturated Zn^{2+} centers in the framework may play a positive role in the affinity of H_2 molecules.[8,11,15,20] The H_2 capacities of **1** and **2** are not particularly high, compared to those observed in other MOFs, such as MOF-505, Cu_2(BPTC) (BPTC = 3,3′,5,5′-biphenyltetracarboxylate), which shows the greatest uptake reported at 77 K and 1 atm (2.47−2.59 wt %).[9,16] Nevertheless, the uptakes of **1** and **2** are comparable with those of highly porous MOFs. For instance, MOF-5, $Zn_4O(BDC)_3$ displays H_2 uptake of 1.3 wt % under the same conditions,[19,24] even though it is far more porous than **1** or **2**. The sorption results and **1** and **2** agree with the recent findings that the high H_2 capacity in MOFs is not necessarily achieved by large surface area and pore volume.[11,15,20] Many factors, such as optimal pore size and coordinatively unsaturated metal centers, need to be considered when designing new MOFs with greater H_2 sorption capacity.

Conclusion

We have synthesized two new three-dimensional metal−organic frameworks on the basis of Zn^{2+} ions, 1,2,4-triazole and naphthalenedicarboxylate where Zn−triazole layers are pillared by dicarboxylate linkers. Gas-sorption experiments revealed that these frameworks have a permanent porosity upon the evacuation of solvents. Although these frameworks possess only moderate H_2 sorption capacities, the results presented indicate that the search for higher H_2 capacity MOFs may concentrate not only on the higher internal surface area materials but also on a combination of optimizable factors such as open metal sites, metal clustering, pore dimensions, and interaction with organic linkers. Our future efforts will be directed toward the design of new MOFs for more effective H_2 storage from careful understanding of the interaction between H_2 molecules and an MOF.

Acknowledgment. This work was supported by the National Science Foundation (DMR-04524444) and Center for Molecular Environment Science (CHE-0221934). H. P. thanks Dr. Yu-Sheng Chen at ChemMatCARS, APS, for his assistance with single-crystal X-ray diffraction and Dr. Yongjae Lee at X7A, NSLS, for his help with powder X-ray diffraction. ChemMatCARS Sector 15 is principally supported by the National Science Foundation/Department of Energy under Grant CHE-0087817. The Advanced Photon Source is supported by the U.S. Department of Energy, Basic Energy Sciences, Office of Science, under Contract No. W-31-109-Eng-38. Use of the National Synchrotron Light Source, Brookhaven National Laboratory, was supported by the U.S. Department of Energy, Office of Science, Office of Basic Energy Sciences, under Contract No. DE-AC02-98CH10886. J. L. and J. Y. L. would like to acknowledge the financial support from the National Energy Technology Laboratory (DE-FC26-05NT42446).

Supporting Information Available: Further details of crystallographic data and H_2 sorption measurements of **1**−**3** and crystallographic information files (CIF) for **1** and **2**. This material is available free of charge via the Internet at http://pubs.acs.org.

CM0623918